International Journal of Science and Research (IJSR)
ISSN (Online): 2319-7064
Index Copernicus Value (2016): 79.57 | Impact Factor (2017): 7.296

Comparative Study of Fuel-Air Mixing in a SPRF and a Conventional Cylindrical Combustor Using a New Unmixedness Index

Amin Lotfiani

[1]Elm-o-fann University College of Science and Technology, Mechanical Engineering Department, Chichest Road, Urmia, Iran

Abstract: ***In diffusion combustion systems, fuel and oxidizer (usually air) are admitted into the combustion chamber in separate streams. In these systems, turbulent mixing of the oxidant with fuel is typically the rate-limiting step of the combustion process. Making any changes to the burner and combustor design to enhance the mixing process can help to tailor the performance of the flame. The stagnation-point reverse-flow (SPRF) combustor is one of the recently-developed combustors which have proven to be efficient. In the present work, a SPRF cylindrical combustor is numerically studied and compared with a conventional one, under isothermal conditions. The importance of this study is the definition of a new simple non-dimensional criterion for assessing the mixing efficiency of burners and combustors, namely, the unmixedness index. This index is used to judge the fuel-air mixture quality in the two combustors. Numerical results are validated against the available experimental data and reasonable agreement is observed. According to the results, the SPRF combustor can improve the fuel-air mixing process in parts of the chamber and the newly-defined unmixedness index can be readily employed to evaluate the fuel-air mixture quality.***

Keywords: Unmixedness index, turbulent mixing, diffusion combustion, SPRF combustor, CFD

1. Introduction

In diffusion combustion systems, fuel and oxidizer (usually air) are admitted into the combustion chamber in separate streams. In these systems, turbulent mixing of the oxidant with fuel is typically the rate-limiting step of the combustion process. Making any changes to the burner and combustor design to enhance the mixing process can help to tailor the performance of the flame. The following is a summary of several studies on turbulent mixing.

Zhdanov et al [1] conducted experiments on the mixing of confined coaxial flows. They measured velocities using a one-component laser Doppler velocimeter and detected scalar field by the laser image fluorescence (LIF) method. The influence of unsteady vortex structures on the mixing was shown. Pallares et al [2] experimentally studied mixing patterns in a fluidized bed. The mixing pattern of a tracer particle was studied in a cold two-dimensional fluidized bed with respect to different influencing parameters. Schumaker [3] made an experimental study of reacting and non-reacting turbulent coaxial jet mixing in a laboratory rocket engine. His study provided very useful data and increased the basic understanding of the complex interaction between turbulent shear flows. Christoffersen [4] studied turbulent mixing in coaxial jets using three-dimensional time-dependent direct numerical simulations (DNS). Mixing was investigated by implementation of a passive scalar in the simulations. Yusaf et al [5] numerically investigated the flow behavior of methane and air in a compressed natural gas (CNG)-air mixer which was designed to be implemented in a CNG-diesel dual-fuel stationary engine. The effect of the number of mixer holes on the mixture quality was evaluated. Semin et al [6] studied a new multi-hole injector nozzle for a sequential port injection CNG engine. Air-fuel mixing and fuel flow velocities was evaluated using computational fluid dynamics (CFD). Souflas and Koutmos [7] compared fuel-air mixing and flame stabilization characteristics of two high-velocity-ratio coaxial jet configurations. Experimental measurements of mixture concentrations and mean temperatures were made to elucidate the relative variations in flame structure and burner performance. Computational simulations of the cold flow fuel-air mixing patterns were also conducted to give an insight into the predominant aerodynamic phenomena involved. Terashima and Koshi [8] presented numerical simulations of nitrogen-hydrogen mixing for a coaxial injector under a supercritical pressure of 10 MPa using a high-order method and studied the effect of outer hydrogen jet temperature. A clear dependence of dense core length on the momentum flux ratio was also demonstrated. Bauer et al [9] carried out experiments on the operational limits of vortex generator premixers (VGPs) with an emphasis on fuel-air mixing at the corresponding high temperatures. The VGP's mixture quality was investigated using particle image velocimetry (PIV) measurements. The influence of the momentum flux ratio on mixture quality was also presented.

In the present work, a stagnation-point reverse-flow (SPRF) cylindrical combustor is numerically studied and compared with a conventional one, under isothermal conditions. The SPRF combustor is one of the recently-developed combustors which have proven to be efficient. The importance of this study is the definition of a new simple non-dimensional criterion, namely, the unmixedness index, for assessing the mixing efficiency of burners and combustors. This index is used to judge the fuel-air mixture quality in the two combustors. Numerical results are validated against the available experimental data and reasonable agreement is observed.

2. Problem Specifications

In this work, two different cylindrical combustors, namely a SPRF and a conventional combustor are studied numerically, under isothermal conditions (cold model). In both the

combustors, fuel (methane) and air are admitted into the combustion (mixing) chamber separately in the form of coaxial turbulent jets. Fuel enters the chamber from a round nozzle and air is admitted through an annulus surrounding the central fuel nozzle. In other words, the coaxial fuel and air nozzles consist of two coaxial pipes with the inner and outer pipe diameters d_1=10 and d_2=50 mm respectively. The coaxial nozzles are mounted on a cylindrical chamber 300 mm in diameter (D=2R) and 1000 mm in length (L). Gases leave the mixing chamber radially through a peripheral slot 10 mm wide in the wall. This slot is adjacent to the end of the chamber opposite the fuel and air nozzles in the conventional combustor and is adjacent to the fuel and air inlet plane in the SPRF combustor as shown in Figure 1. Air and fuel average inlet velocities (at the nozzle exit) are 10 and 20 m/s respectively. The corresponding air-to-fuel momentum ratio is 10.98 and the overall fuel-to-air equivalence ratio is 0.782. Reynolds number based on the fuel jet parameters is 12738.

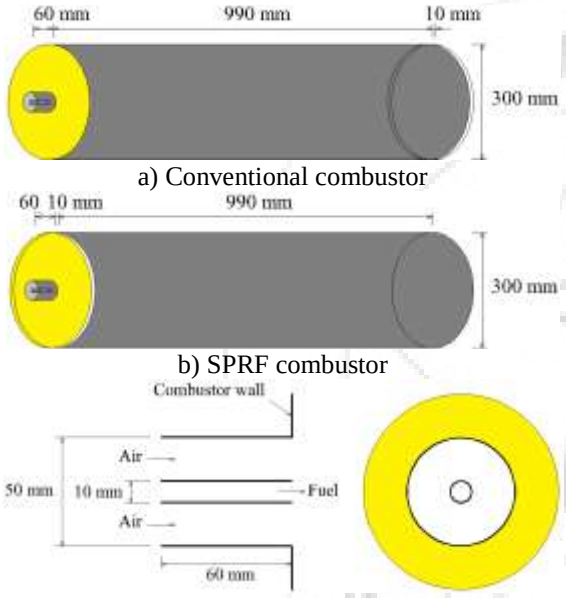

Figure 1: Dimensions of the two combustors, the coaxial air and fuel nozzles and the peripheral outlet

3. Modeling and Computations

The mathematical model is based on the solution of the continuity, momentum, and turbulence model equations as well as the chemical species transport equations. Turbulent viscosity is determined using the two-equation Realizable k-ε model because this model addresses the deficiencies of the traditional k-ε models. For example, the Realizable k-ε model satisfies certain mathematical constraints on the normal stresses, consistent with the physics of turbulent flows. The modeled equation for the dissipation rate ε and the eddy-viscosity formula are also improved in the Realizable k-ε model. Thus the performance of this model is substantially better than that of the traditional k-ε models, especially for flows involving rotation, recirculation, strong streamline curvature and planar and round jets [10]-[13].

The calculations are carried out using the flow solver Fluent based on the finite volume method. All the governing equations are discretized using the second order upwind scheme. The discretized equations are solved using the Simple algorithm. The implicit and segregated solver is applied for the solution of the system of governing equations. The software Gambit is employed to generate the geometry and mesh for the computational domain. As indicated in [14], two-dimensional and three-dimensional simulations of turbulent mixing in the cases of interest provide virtually identical results. Hence, all the cases are simulated two-dimensionally using the axisymmetric solver. This helps reduce the computational effort, without compromising the accuracy. Computations are performed on three progressively finer meshes in order to secure grid independence. The chosen mesh for both the combustors, namely the conventional and the SPRF combustor, consists of 12848 quadrilateral cells. To capture the details of the flow accurately, the size of the cells are reduced near the air and fuel inlets and the combustor walls where large gradients are expected. An example of the generated meshes is shown in Figure 2.

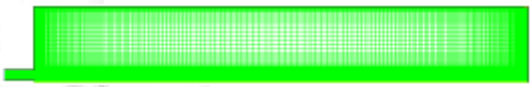

Figure 2: An example of the computational grids consisting of 12848 quadrilateral cells

Velocity inlet boundary condition is used at the fuel and air inlets and pressure outlet boundary condition is used at the combustor outlet. Wall boundary condition with constant temperature of 300 K and no-slip condition is used at the walls. Convergence criterion for all the governing equations is the scaled residual value. Solution is considered to be converged when the scaled residual values become less than 1.7×10^{-6}. Turbulence intensity is assumed to be 10% at the fuel and air inlets and also at the peripheral outlet.

In order to judge the mixture quality, a new simple non-dimensional unmixedness index Λ is defined by the author as

$$\Lambda(\%) = \frac{100}{2}\left(\left|f_{avg} - f_{overall}\right| + \frac{1}{A_t}\sum_{i=1}^{n} A_i\left|f_i - f_{avg}\right|\right) \quad (1)$$

where f is a conserved scalar known as the mixture fraction and n is the number of computational cells in the desired cross-section. The same definition of the mixture fraction is used as is given in [10], i.e.:

$$f = \frac{Z_j - Z_{j,ox}}{Z_{j,fuel} - Z_{j,ox}} \quad (2)$$

In the above definition, Z_j is the elemental mass fraction for element j, the subscript ox denotes the value at the oxidizer stream inlet and the subscript fuel denotes the value at the fuel stream inlet. If the diffusion coefficients for all species are equal, then Equation (2) is identical for all elements and the mixture fraction definition is unique. The mixture fraction is thus the elemental mass fraction that originated from the fuel stream.

In Equation (1), the subscript avg stands for the cell face area-weighted average in the desired cross-section and A_t is the total area of the cross-section of interest. Λ can be evaluated at any desired cross-section of the combustor. The

first term in the right-hand side of the above definition, represents the relative deviation of the average mixture fraction at the desired cross-section from the overall mixture fraction. The second term shows the average deviation of the local mixture fraction at the cross-section of interest from the average mixture fraction at that cross-section. Both the terms are important in assessing the mixing efficiency of a system. In the ideal case, the local mixture fraction at the desired cross-section uniformly equals the overall mixture fraction and the unmixedness index becomes zero. This corresponds to a completely stirred fuel and air mixture. In general, Λ can vary between 0 and 100%.

4. Results and Discussion

Numerical results are validated against the measurements of Warda et al [15] in the developing region and the experimental data of Champagne and Wygnanski [16] in the fully-developed region of coaxial air jets. The inner-to-outer jet exit velocity ratio studied by Warda et al was 10.0/5.0 (m/s) and d_1/d_2=8/18 (mm). Reynolds number based on the inner jet parameters was 5100. Champagne and Wygnanski measured velocity profiles for d_1=25.4 mm and the outer-to-inner nozzle area ratio of 2.94. The outer-to-inner jet exit velocity ratio was 0.25 and Reynolds number based on the inner jet parameters was 10^5.

Figures 3-a and 3-b show the axial velocity decay along the centerline of the coaxial air jets. Figure 3-c shows the radial distribution of the axial velocity at x/d_1=9.25. As can be seen in these figures, axial distance from the inner nozzle exit is nondimensionalized by the inner nozzle diameter d_1, axial velocity by the inner jet exit velocity or by the centerline velocity, and radial distance from the centerline, r, by the jet half-width for velocity b_v (where the axial velocity is reduced to half of that on the centerline).

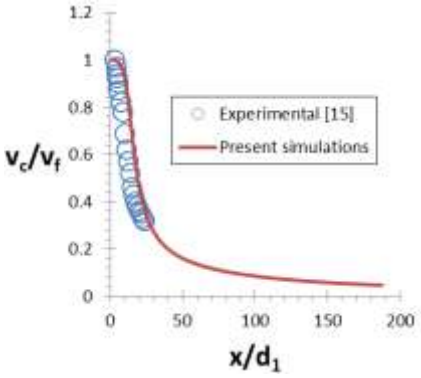

(a)

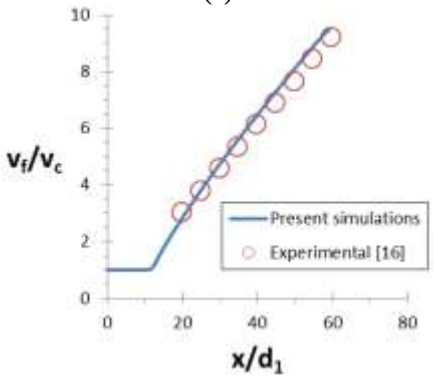

(b)

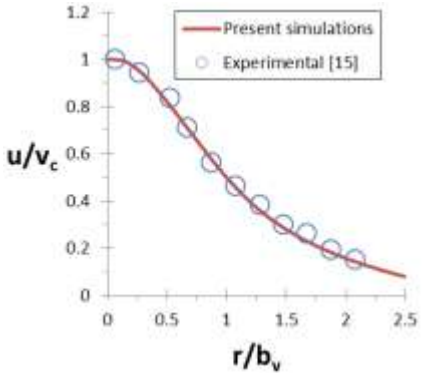

(c)

Figure 3: Comparison of simulated and measured velocity profiles for coaxial air jets to validate the simulation procedure, a) Axial velocity along the centerline in the developing region; b) Axial velocity along the centerline in the fully-developed region; c) Radial distribution of the axial velocity at x/d_1=9.25

Contours of stream function are shown in Figure 4. Recirculating regions and flow pattern in the two combustors are demonstrated in this figure. As can be seen, recirculation is larger and stronger in the conventional combustor compared to the SPRF combustor.

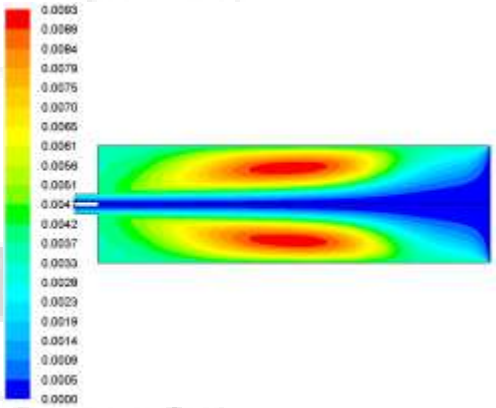

a) Conventional combustor

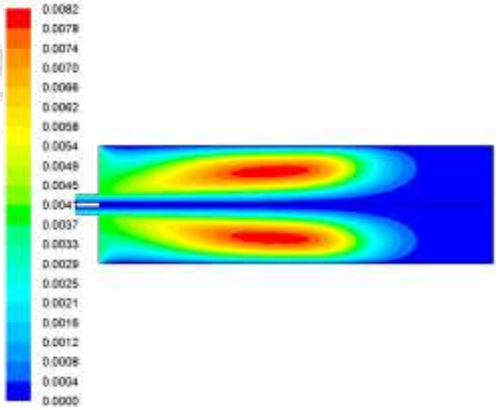

b) SPRF combustor

Figure 4: Contours of stream function (kg/s): a) in the conventional combustor; b) in the SPRF combustor

Changes in the axial velocity u along the centerline of the two combustors with the axial distance from the fuel nozzle exit x are compared in Figure 5-a. As can be seen, the axial velocity on the centerline decays faster in the SPRF combustor, especially at the end of the combustor (after x/L=0.5), compared to the conventional one. This is due to

the reverse flow created in the SPRF combustor. In this figure, the axial distance from the fuel nozzle exit x is nondimensionalized by the length of the combustion chamber L, and the axial velocity u by the fuel jet exit velocity v_f. Figure 5-b shows changes in the nondimensional radial velocity along the centerline of the two combustors with the nondimensional axial distance from the fuel nozzle exit. As is obvious, the radial velocity component in the SPRF combustor is larger than that in the conventional one between x/L=0.4 and x/L=0.7 and smaller after x/L=0.7. Figure 5-c demonstrates variations in the mixture fraction along the centerline of the two combustors. The two curves are almost identical and no significant difference is observed.

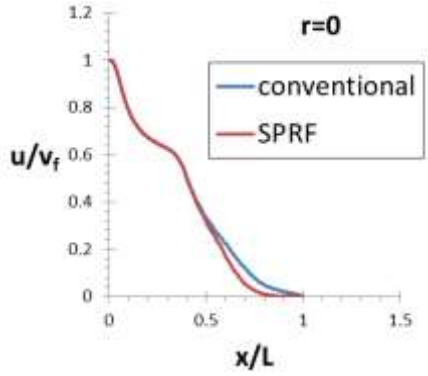

a) Axial velocity along the centerline of the two combustors

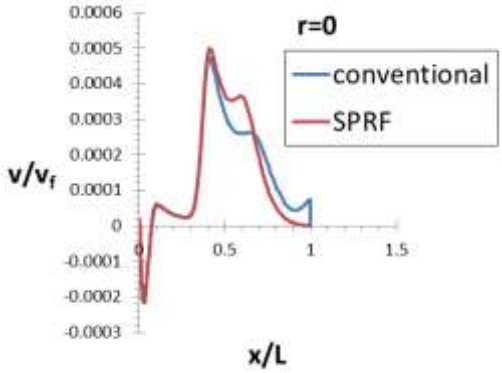

b) Radial velocity along the centerline of the two combustors

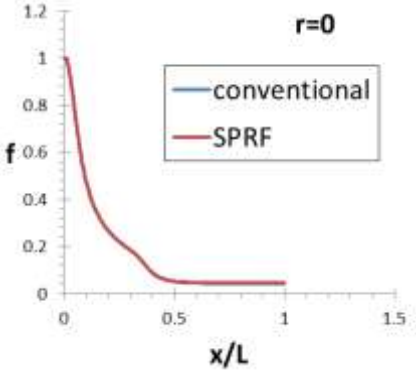

c) Mixture fraction along the centerline of the two combustors

Figure 5: Variations in the velocity components and the mixture fraction on the centerline of the two combustors

Radial distribution of the velocity components and the mixture fraction at several cross-sections of the two combustors can provide a clear understanding of the flow and mixing. For instance, four different cross-sections along the centerline of the two combustors, namely x/L=0.10, 0.40, 0.60, and 0.90 are chosen to study the radial distributions of interest. Radial distributions of the axial velocity at the chosen cross-sections are shown in Figure 6 for the two combustors. The radial distance from the centerline of the combustors r is nondimensionalized by the radius of the combustion chamber R.

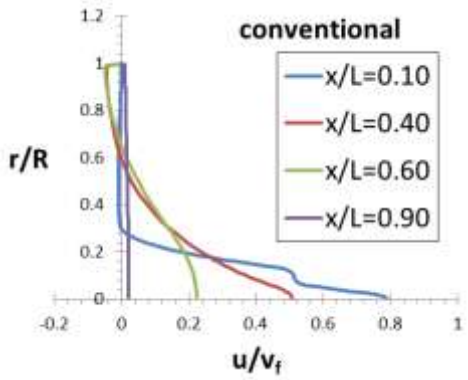

a) Conventional combustor

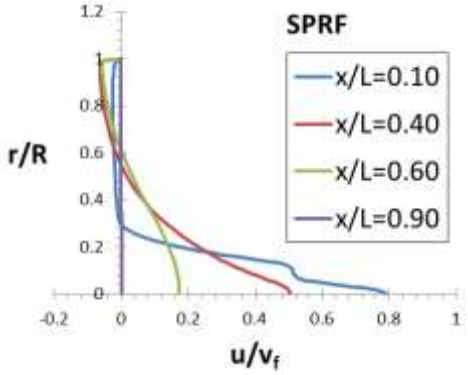

b) SPRF combustor

Figure 6: Axial velocity profiles at different cross-sections along the centerline of the two combustors

It is observed that in the conventional combustor, in contrast to the SPRF combustor, reverse flow at x/L=0.10 is not noticeable. Radial distributions of the radial velocity at different cross-sections are demonstrated in Figure 7 for the two combustors. It can be seen that in the SPRF combustor, the radial velocity components are considerably larger at x/L=0.60 and smaller at x/L=0.90 compared to the conventional combustor. The latter is due to the stagnation region created at the end of the SPRF combustion chamber.

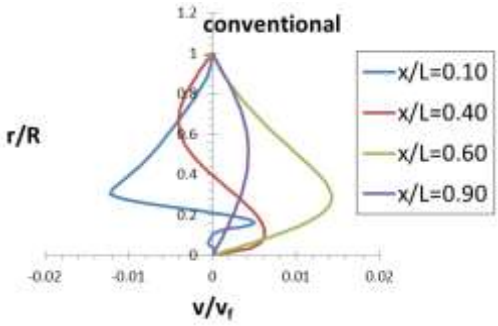

a) Conventional combustor

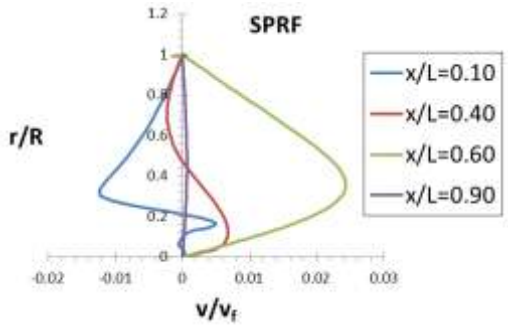

b) SPRF combustor

Figure 7: Radial distribution of the radial velocity at different cross-sections along the centerline of the two combustors

Figure 8 shows radial distributions of the mixture fraction at different cross-sections along the centerline of the two combustors. Obviously, there is no noticeable difference between the distributions of the mixture fraction in the two combustors.

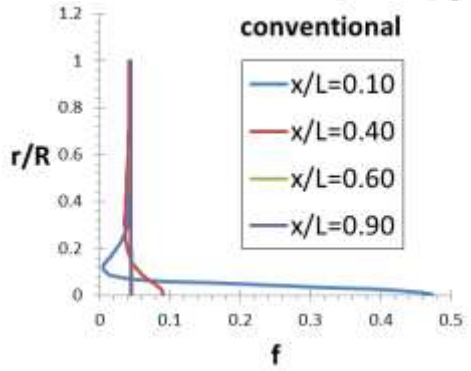

a)Conventional combustor

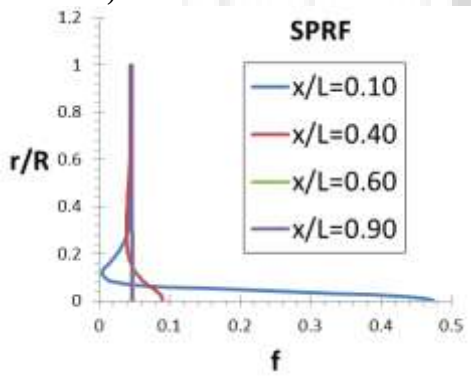

b) SPRF combustor

Figure 8: Radial distribution of the mixture fraction at different cross-sections along the centerline of the two combustors

In order to compare the two combustors more clearly, radial distributions of the velocity components and the mixture fraction are shown again in Figures 9 to 11, this time with the velocities being nondimensionalized by the maximum velocity (i.e. velocity on the centerline at the cross-section of interest) and the mixture fraction being nondimensionalized by the maximum mixture fraction (i.e. mixture fraction on the centerline at the cross-section of interest). Figure 9 shows radial distributions of the axial velocity at different cross-sections for the two combustors. It can be inferred from this figure that the reverse flow generated in the SPRF combustor is stronger than that in the conventional combustor. In the conventional combustor, no reverse flow is observed at x/L=0.90 in contrast to the SPRF combustor.

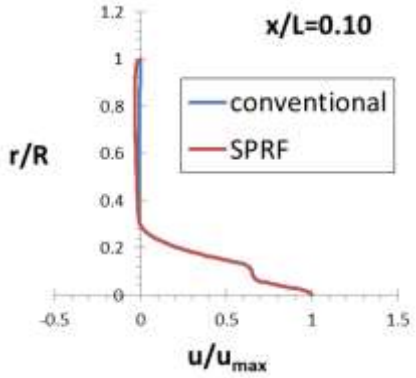

a) x/L=0.10

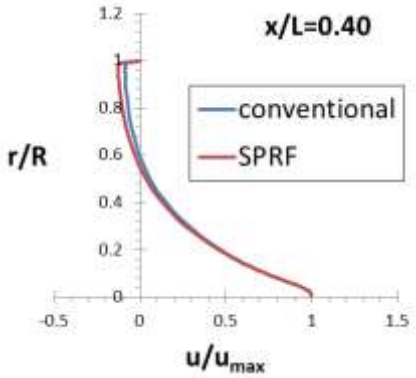

b) x/L=0.40

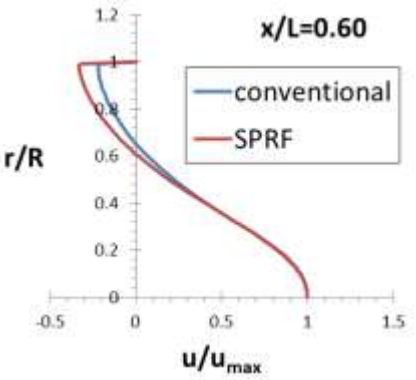

c) x/L=0.60

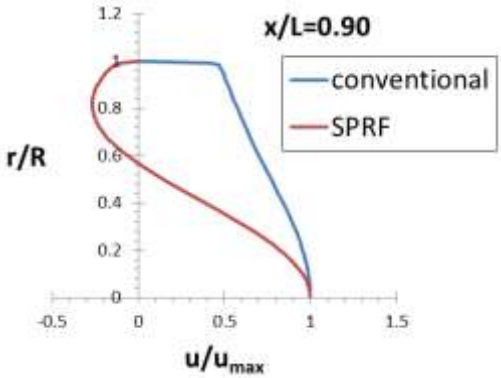

d) x/L=0.90

Figure 9: Axial velocity profiles at different cross-sections along the centerline of the two combustors

Figure 10 demonstrates radial distributions of the radial

velocity at different cross-sections for the two combustors. No significant difference between the distributions of the radial velocity is observed in the two combustors. Radial flow towards the centerline of the conventional combustor is stronger than that in the SPRF combustor at x/L=0.40.

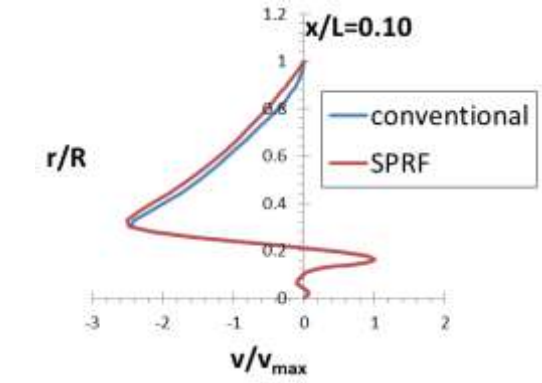

a) x/L=0.10

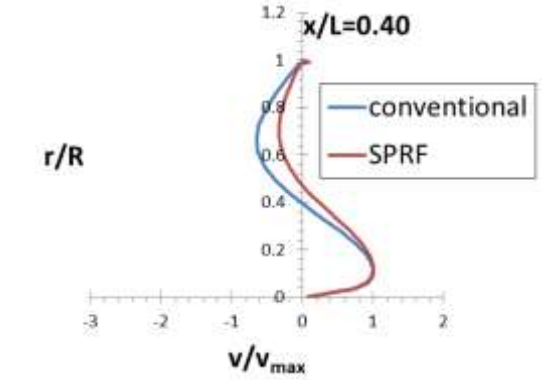

b) x/L=0.40

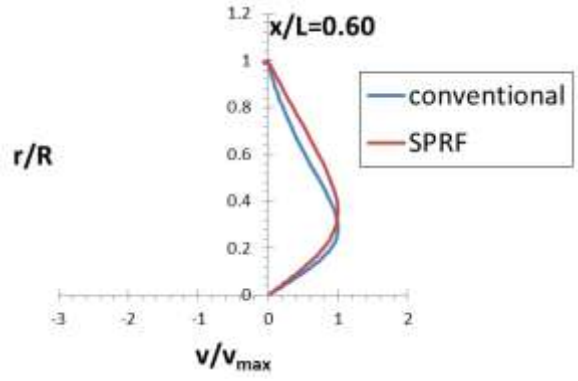

c) x/L=0.60

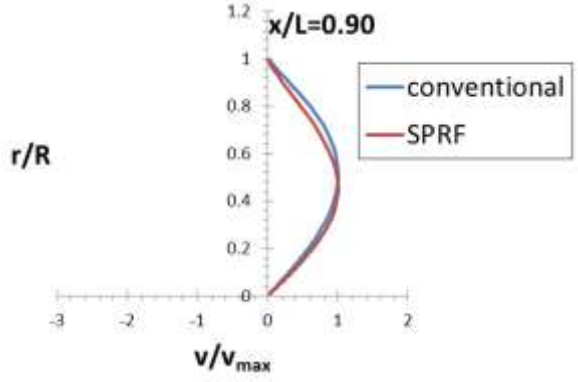

d) x/L=0.90

Figure 10: Radial distributions of the radial velocity at different cross-sections along the centerline of the two combustors

Radial distributions of the mixture fraction at different cross-sections along the centerline of the two combustors are shown in Figure 11. From this figure, it can be found out that radial distributions of the mixture fraction in the two combustors are virtually identical near the fuel and air inlet plane (x/L=0.10) and also at the end of the combustors (x/L=0.90). However, the mixture fraction values are higher in the SPRF combustor compared to the conventional combustor, in the middle part of the combustion chamber (x/L=0.40 and 0.60).

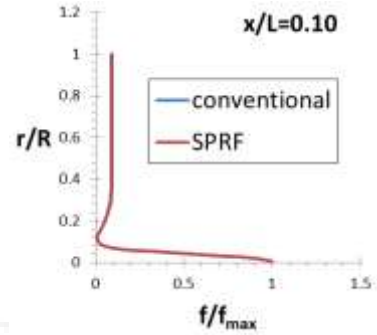

a) x/L=0.10

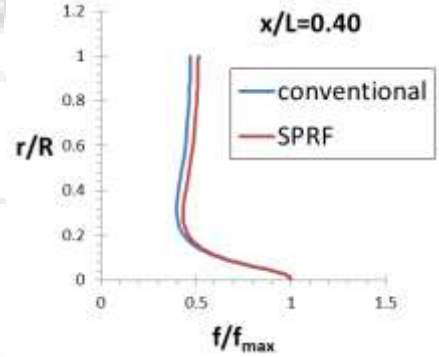

b) x/L=0.40

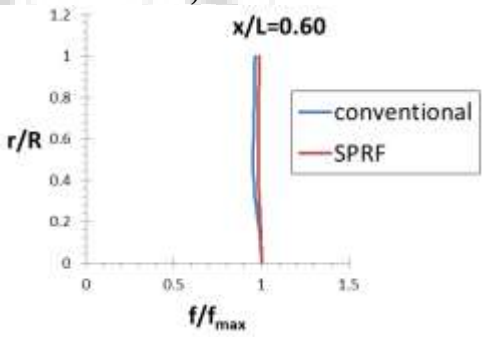

c) x/L=0.60

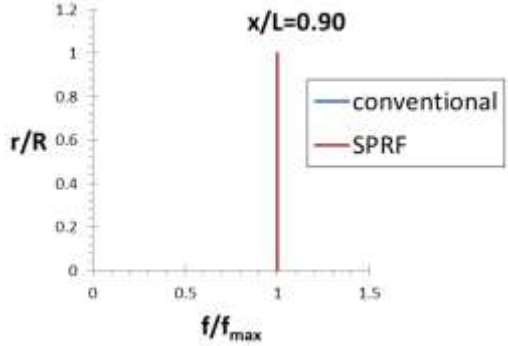

d) x/L=0.90

Figure 11: Radial distributions of the mixture fraction at different cross-sections along the centerline of the two combustors

The unmixedness index Λ is calculated from Equation (1) at the chosen cross-sections to judge the mixing performance of the two combustors. The calculated values are shown in Figure 12. As can be seen from this figure, the unmixedness index values in the SPRF combustor are lower than those in the conventional combustor, in the first half of the cylindrical chamber (i.e. 0<x/L<0.50). The reverse is true for the second half (i.e. 0.50<x/L<1.00). The calculated values of unmixedness index are given in Table 1.

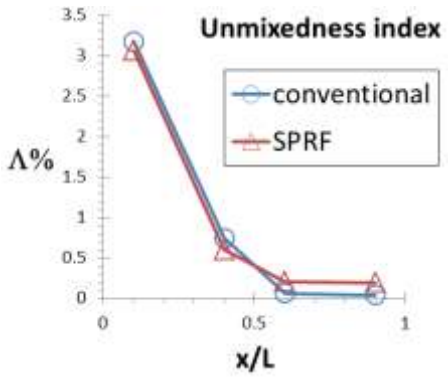

Figure 12: Unmixedness index Λ calculated at different cross-sections to judge the mixing performance of the two combustors

Table 1: Values of the unmixedness index Λ calculated at different cross-sections of the two combustors

	x/L=0.10	x/L=0.40	x/L=0.60	x/L=0.90
Conventional	3.1734	0.7444	0.0624	0.0385
SPRF	3.0600	0.6014	0.2065	0.1962

According to the values of the unmixedness index given above, it can be concluded that the SPRF combustor is more efficient in mixing the fuel and air streams at x/L=0.10 and 0.40 compared to the conventional combustor. However, at the two other cross-sections, namely x/L=0.60 and 0.90 the conventional combustor is more efficient. This might be due to the larger and stronger recirculation in the conventional combustor (see Figure 4) which provides rapid contact between fuel and air, entrains lean and rich zones and blends them together, especially in the second half of the cylindrical chamber (after x/L=0.50).

5. Conclusions

In the present work, a SPRF cylindrical combustor is numerically studied and compared with a conventional combustor, under isothermal conditions. The importance of this study is the definition of a new simple non-dimensional criterion for assessing the mixing performance of burners and combustors, namely, the unmixedness index. This index is used to judge the fuel-air mixture quality in the two combustors. Numerical results are validated against the available experimental data and reasonable agreement is observed. According to the results, the SPRF combustor can improve the fuel-air mixing process in parts of the chamber, i.e. in the first half of the cylindrical chamber (0<x/L<0.50). However, the conventional combustor performs better in the second half of the chamber (0.50<x/L<1.00). As illustrated, the newly-defined unmixedness index can be readily employed to evaluate the mixing efficiency of the combustors.

References

[1] V. Zhdanov, N. Kornev, E. Hassel, A. Chorny, "Mixing of Confined Axial Flows,"International Journal of Heat and Mass Transfer, 49 (21-22), pp. 3942-3956, 2006.
[2] D. Pallares, P. A. Diez, F. Johnsson, "Experimental Analysis of Fuel Mixing Patterns in a Fluidized Bed," In Proceedings of the 12thInternational Conference on Fluidization-New Horizons in Fluidization Engineering, pp. 929-936, 2007.
[3] S. A. Schumaker, An Experimental Investigation of Reacting and Non-reacting Coaxial Jet Mixing in a Laboratory Rocket Engine, Ph.D. Thesis, University of Michigan, 2009.
[4] I. M. Christoffersen, A Numerical Study of Turbulent Mixing in Coaxial Jets, M.S. Thesis, Norwegian University of Science and Technology, Trondheim, 2010.
[5] T. Yusaf, P. Baker, I. Hamawand, M. M. Noor, "Effect of Compressed Natural Gas Mixing on the Engine Performance and Emissions,"International Journal of Automotive and Mechanical Engineering (IJAME), 8, pp. 1416-1429, 2013.
[6] Semin, B. Cahyono, Amiadji, R. A. Bakar, "Air-fuel Mixing and Fuel Flow Velocity Modeling of Multi Holes Injector Nozzle on CNG Marine Engine,"Procedia Earth and Planetary Science, 14, pp. 101-109, 2015.
[7] K. Souflas, P. Koutmos, "Flow, Mixing, and Combustion Characteristics of High Velocity Ratio Plane Coaxial and Convoluted Trailing Edge Nozzles,"Journal of Energy Engineering, 2016, doi: 10.1061/(ASCE)EY.1943-7897.0000408.
[8] H. Terashima, M. Koshi, "Numerical Simulations of Mixing under Supercritical Pressures of a Shear Coaxial Injector using a High-order Method: Effect of Outer Jet Temperature,"Progress in Propulsion Physics, 8, pp. 25-42, 2016.
[9] S. Bauer, S. Babler, B. Hampel, Ch. Hirsch, Th. Sattelmayer, "Mixture Quality of a Vortex Generator Premixer and Alternative Premixer Designs in the Auto-ignition Regime of Hydrogen Air Flames,"In Proceedings of the ASME Turbo Expo 2017: Turbomachinery Technical Conference and Exposition, Paper code GT2017-64154, 13 pages, 2017, doi: 10.1115/GT2017-64154.
[10] Fluent 6.2 User's Guide, Fluent Inc., Lebanon, NH 03766, 2005.
[11] Sh. Khalilarya, N. Pourmahmod, A. Lotfiani, "Evaluation of Two-equation Turbulence Models for the Simulation of Gaseous Round Jets," In Proceedings of the Mechanical Engineering Conference (MEC2009), pp. 210-211, 2009.
[12] A. Lotfiani, Sh. Khalilarya, S. Jafarmadar, "A Semi-analytical Model for the Prediction of the Behavior of Turbulent Coaxial Gaseous Jets,"Thermal Science, 17 (4), pp. 1221-1232, 2013.
[13] A. Lotfiani, "Evaluation of Two-equation k-εTurbulence Models for the Simulation of Plane Turbulent Wall Jets," In Proceedings of the National Conference on Novel Research in Science and Engineering, Paper code CE-0370, 2017.

[14] Sh. Khalilarya, A. Lotfiani, "A New Burner Layout for the Enhancement of Mixture Formation in Furnaces,"In Proceedings of the 19th Annual Conference on Mechanical Engineering ISME2011, p. 3, 2011.
[15] H. A. Warda, S. Z. Kassab, K. A. Elshorbagy, E. A. Elsaadawy, "Influence of the Magnitude of the Two Initial Velocities on the Flow Field of a Coaxial Turbulent Jet,"Flow Measurement and Instrumentation, 12, pp. 29-35, 2001.
[16] F. H. Champagne, I. J. Wygnanski, "An Experimental Investigation of Coaxial Turbulent Jets,"International Journal of Heat and Mass Transfer, 14, pp. 1445-1464, 1971.

Author Profile

AminLotfiani received the B.S., M.S. andPh.D. degrees in Mechanical Engineering from Urmia University in 2005, 2007 and 2012, respectively. His Ph.D. thesis work focused on coaxial gaseous jets and flow characteristics in tangentially-fired furnaces with gaseous fuel. He is now a faculty member of the mechanical engineering department in Elm-o-fann University College of Science and Technology in Urmia.